Supporting Information for Dynamic Clustering in Suspension of Motile Bacteria

Xiao Chen,[1] Xiang Yang,[1] Mingcheng Yang,[2] and H. P. Zhang[1,*]

[1] *Department of Physics and Astronomy and Institute of Natural Sciences, Shanghai Jiao Tong University, China*

[2] *Beijing National Laboratory for Condensed Matter Physics and Key Laboratory of Soft Matter Physics, Institute of Physics, Chinese Academy of Sciences, China*

(Dated: June 11, 2015)

Abstract

This document contains supporting information for an article titled "Dynamic Clustering in Suspension of Motile Bacteria"

* To whom correspondence should be addressed: hepeng_zhang@sjtu.edu.cn

IMAGE ANALYSIS AND CLUSTER IDENTIFICATION

Part of a raw image from experiments is shown in Fig. S1(a); bacteria appear as white blobs. We extract centers of mass and orientations of more than 85% of all bacteria, then track bacterial motion in time by a standard algorithm based on a minimum distance criterion between bacteria in successive frames[1]. From the trajectories, we compute translational and rotational velocities.

Bacteria are grouped into clusters based on local position information. We use Delaunay triangulation to identify neighboring bacteria (Fig. S1(b)) and compute areas of Voronoi cells occupied by individual bacterium (Fig. S1(c)). We define two neighboring bacteria as members of the same cluster if their Voronoi cell areas are smaller than S_d=4.9 μm^2. This operation can correctly assign majority of bacteria into clusters. However, bacteria at the edge of a cluster often occupy Voronoi cells larger than S_d=4.9 μm^2 therefore are not correctly assigned. To correct this problem, in each video frame, we search around assigned bacteria for bacteria at the edge. For an assigned bacterium at $\vec{r}_{i,I}$ (the ith bacterium in the Ith cluster), we assign any un-assigned bacterium whose distance from $\vec{r}_{i,I}$ is less than R_d= 2.5 μm to the Ith cluster. To track clusters in time, we consider two clusters that are in adjacent video frames and share more than 60% common constituent bacteria to be the same cluster.

We use radial distribution function (RDF) as a guide to select appropriate values for R_d and S_d. As shown in Fig. S2(a), the first peak of radial distribution function extends approximately to R_d= 2.5 μm. S_d = 4.9 μm^2 is the area of a circle with a diameter of R_d. Statistical properties of extracted clusters depend weakly on the particular values of R_d and S_d around the chosen ones, as shown by cluster size distributions in Fig. S2(b), cluster translational speed in (c), rotational period in (d), and examples of clusters extracted with different parameters in (e-g) .

FLUID DYNAMIC CALCULATION

We use the Regularized Stokeslet method [2] to compute flow fluid generated by a model bacterium oriented perpendicular to the interface (cf. Fig. 2(a)). We represent the cell body with a sphere and the flagellar bundle with a single helical flagellum. Similar models have

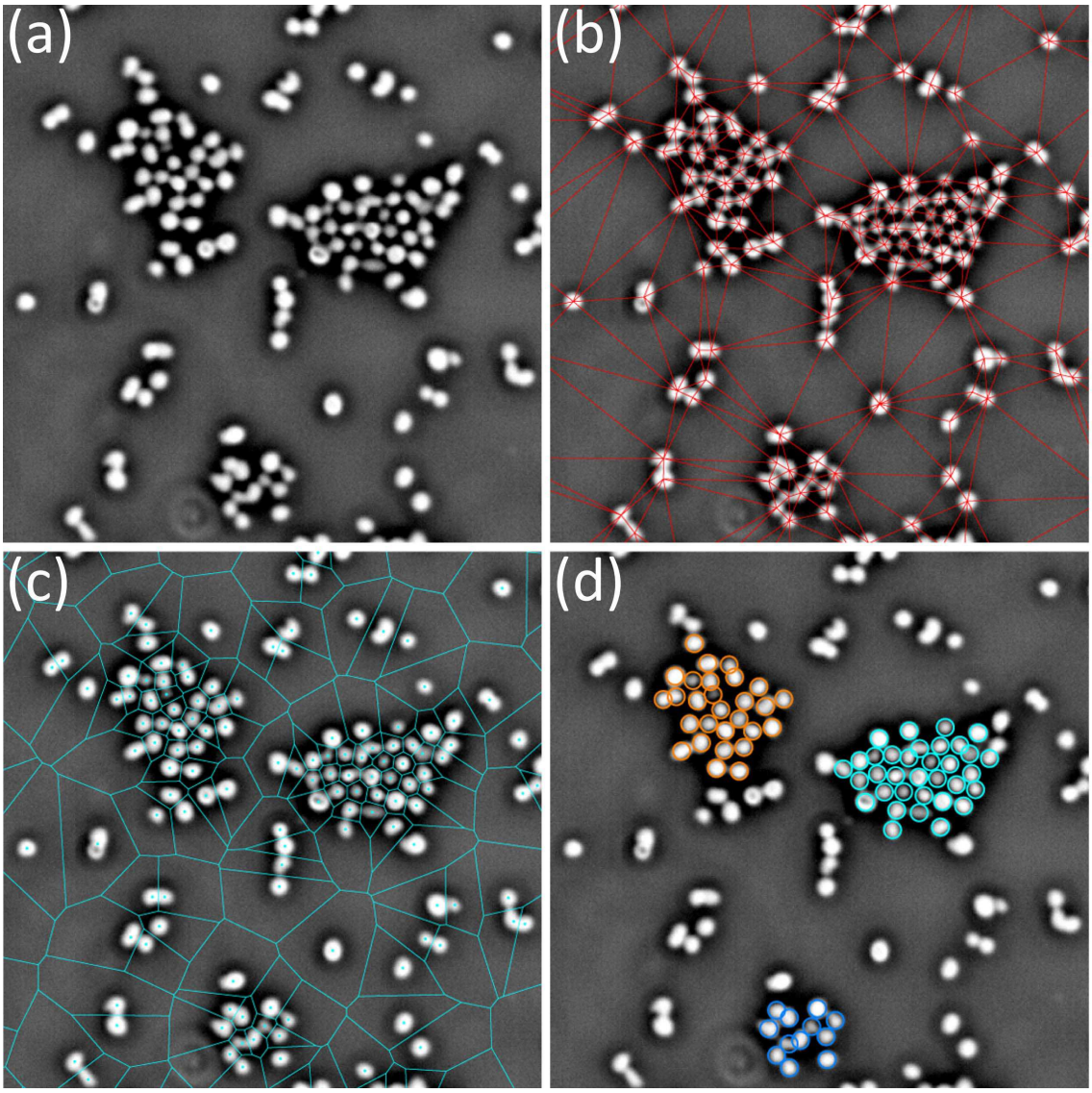

FIG. S1. Procedure to identify clusters. (a) Part of a raw experimental image(500×500 pixels^2). (b) Delaunay triangulation identifies neighboring bacteria. (c) Voronoi cells plotted on the original image. (d) Identified bacteria clusters shown by color-code.

been used extensively in the literature [3–5]. Surface of the cell body (1 μm in diameter) is covered by 2562 uniformly distributed Stokeslets and nearest points are separated by $\Delta_b = 0.14$ μm. The centreline of flagellum is given by:

$$\vec{r}\,(s) = -s\hat{k} + \left(1 - e^{-s^2/k_E^2}\right) h \left(\cos\left(2\pi s/\lambda\right)\hat{i} + \sin\left(2\pi s/\lambda\right)\hat{j}\right),$$

where the pitch$\lambda = 2.2$ μm, coil radius $h = 0.2$ μm, $k_E = 3/\lambda$ determines the length of the tapering region, and s is the distance along the axis of the helix, ranging from 0 to

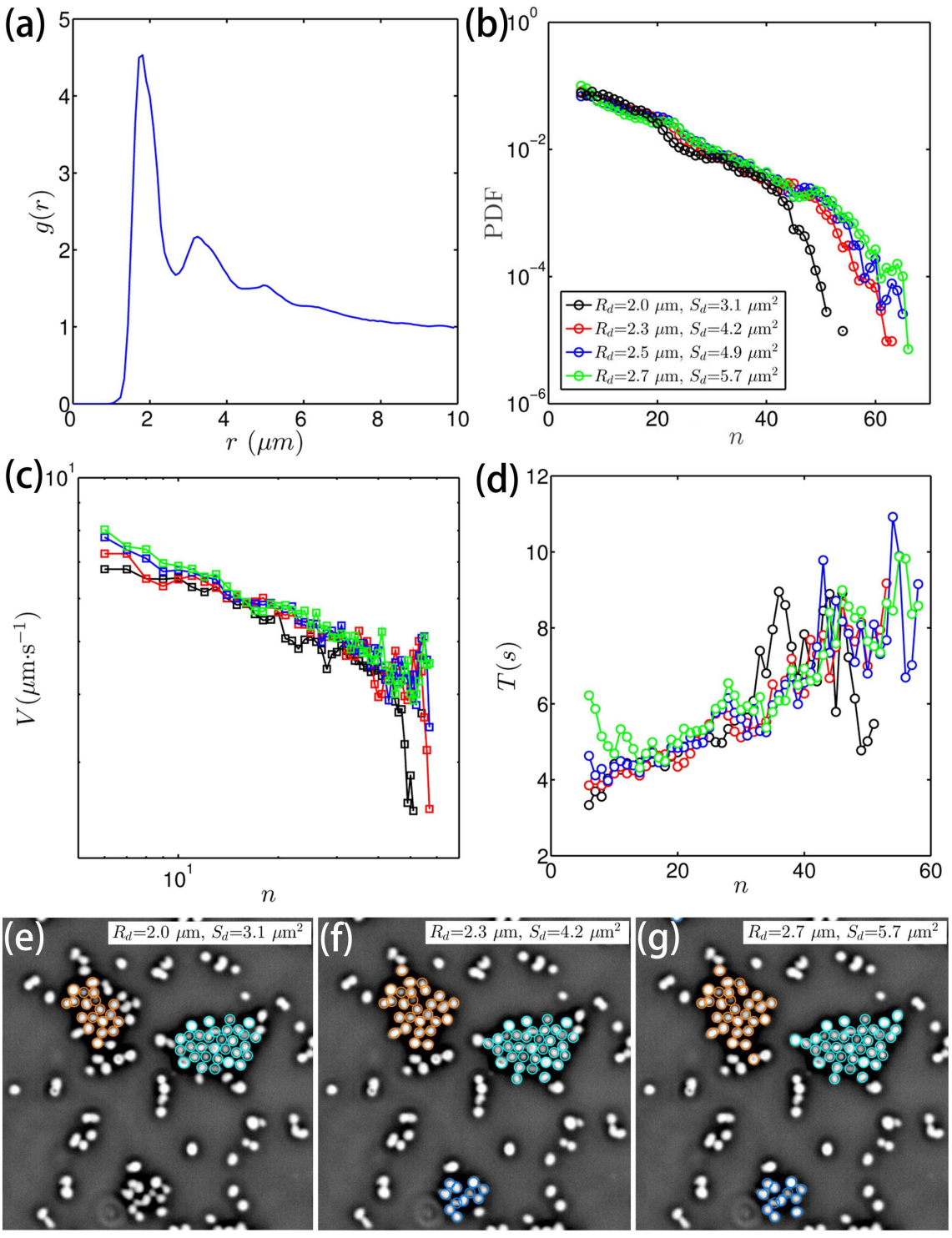

FIG. S2. Selection and sensitivity tests for R_d and S_d used in cluster identification. (a) Radial distribution function (RDF) measured at density ϕ= 0.044 μm^{-2}. The first peak of RDF appears at r=1.7μm. (b-d) Cluster size distributions, mean translation speed, and mean rotation period as functions of cluster size computed with four different sets of parameters (R_d and S_d) at density ϕ= 0.044 μm^{-2}. (e-g) Examples of clusters identified under different sets of parameters.

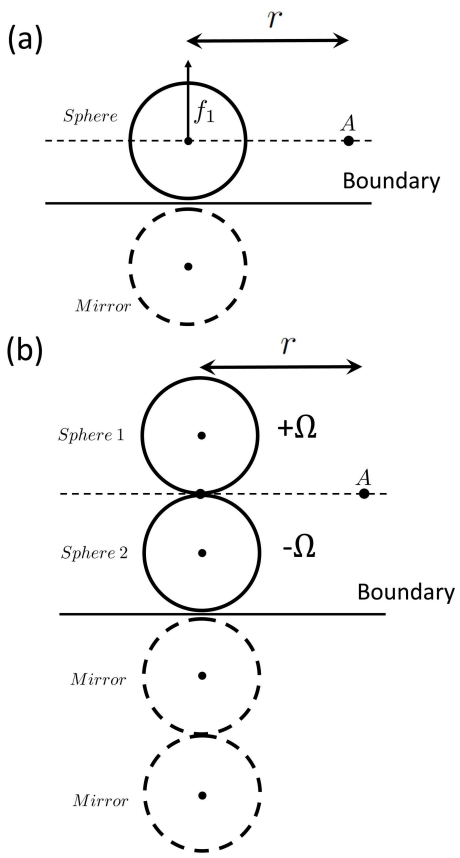

FIG. S3. Models used to derive analytical expressions for radial (a) and tangential (b) velocity components. Gap between models and the boundary is assumed to be infinitely small.

the axial length of 6.6 μm. The flagellum base is separated from the cell body by a gap of 0.1 μm. We discretize the surface of the helical flagellum with cross sections along its length and use 6 regularized Stokeslets on the perimeter of each circular cross section [6]. We separate adjacent cross sections by a distance equal to the filament radius $a = 0.02$ μm. Following Ref. [5], we use 0.14 μm and 0.02 μm as the Regularization parameters for Stokeslets on the cell body and flagellum, respectively. Variations in grid spacing and the Regularization parameter around the chosen values lead to a few percents changes in final flow fields; observed flow features and scalings remain robust. No-slip boundary condition is required on the surface of the bacterium. A free-slip boundary condition at the interface ($z = 0$) is realized through an imaging method[7].

The cell body rotates with an angular velocity of $\Omega_z = -60$ rad/s and the flagellum rotates in the opposite sense with an angular velocity set by the torque balance in the z direction. Other translational and rotational degrees of freedom are frozen for the body and

the flagellum. Gap between the body and the interface is set to be 50 nm which is close a lengthscale estimated by balancing the propulsive force, f_z, generated by the bacterium in z direction with thermal excitation: $\xi = \frac{k_b T}{|f_z|}$. Under the conditions listed above, we find $f_z = -0.11$ pN and this leads to the lengthscale: $\xi \backsimeq 40$ nm. Simulations are also carried out with other gap values; flow features and scalings similar to those in Fig. 2 are observed. We note that flow fields in Fig. 2 are obtained by averaging instantaneous fields over a rotating period [4].

PARAMETRIZED EXPRESSIONS FOR RADIAL AND TANGENTIAL FLOW COMPONENTS

We derive analytical expressions that can be used to parametrize radial and tangential flow velocities in the inset of Fig. 2(b). Models used to derive analytical expressions are shown in Fig. S3; mirroring particles are used to obtain free-slip boundary condition at the boundary. For the radial component, we model the bacterium as a sphere with an effective radius S_1. As shown in Fig. S6 (a), the sphere applies a force f, perpendicular to the interface, on the fluid. The velocity field generated by the sphere can be obtained by solving the Stokes equations together with the following boundary conditions: (1) the velocity field is vanishing at infinity, (2) the normal component of the velocity field vanishes at the sphere surface, (3) the total stress integrated over the sphere surface corresponds to f . We consider a point, A, which is r away from the center of the bacterium. Radial velocity at A can be obtained by summing fluid flow generated by the sphere and its mirror image:

$$V_{rad}\left(r\right) = \frac{f S_1}{8\pi\eta}\left[-\frac{r}{\left(r^2+4S_1^2\right)^{\frac{3}{2}}} + \frac{3S_1^2 r}{4\left(r^2+4S_1^2\right)^{\frac{5}{2}}}\right], \tag{S1}$$

where η is the fluid viscosity. For the tangential flow generated by rotational motion, we model the bacterium as two counter-rotating spheres with an effective radius S_2 and each sphere is treated as a Rotlet[8]. For point A, r away from the bacterium, we obtain the tangential flow:

$$V_{tan}\left(r\right) = \frac{S_2^3\Omega}{2}\left[\frac{r}{\left(r^2+9S_2^2\right)^{\frac{3}{2}}} - \frac{r}{\left(r^2+25S_2^2\right)^{\frac{3}{2}}}\right]. \tag{S2}$$

Treating f, S_1, Ω, and S_2 as fitting parameters, we can use Eq. S1 and Eq. S2 to fit velocity fields from the Regularized Stokeslet calculations. As shown in the insert of Fig. 2(b), fitting

quality is excellent and parameters obtained are: $f = 0.6$ pN, $S_1 = 1.67$ μm, $\Omega = 134$ rad/s, and $S_2 = 0.7\mu$m.

---

[1] H. P. Zhang, A. Be'er, E. L. Florin, and H. L. Swinney, Proc. Natl. Acad. Sci. U. S. A. **107**, 13626 (2010).

[2] R. Cortez, L. Fauci, and A. Medovikov, Phys. Fluids **17**, 031504 (2005).

[3] M. RAMIA, D. L. TULLOCK, and N. PHANTHIEN, Biophys. J. **65**, 755 (1993).

[4] H. Shum, E. A. Gaffney, and D. J. Smith, Proceedings of the Royal Society A-mathematical Physical and Engineering Sciences **466**, 1725 (2010).

[5] Y. Hyon, Marcos, T. R. Powers, R. Stocker, and H. C. Fu, J. Fluid Mech. **705**, 58 (2012).

[6] B. Rodenborn, C. H. Chen, H. L. Swinney, B. Liu, and H. P. Zhang, Proc. Natl. Acad. Sci. U. S. A. **110**, E338 (2013).

[7] R. Di Leonardo, D. Dell'Arciprete, L. Angelani, and V. Iebba, Phys. Rev. Lett. **106**, 038101 (2011).

[8] S. Kim and J. S. Karilla, *Microhydrodynamics: Principles and Selected Applications* (Butterworth-Heinemann, Boston, MA,, 1991).